Scanning Electron Microscopy

Volume 1985 | Number 3 Article 5

6-26-1985

Ion Discrimination Effects in the Laser Microprobe Mass Analyzer

Eric Michiels
University of Antwerp

Marc De Wolf
University of Antwerp

Renaat Gijbels
University of Antwerp

SCANNING ELECTRON MICROSCOPY/1985/III (Pages 947-958)
SEM Inc., AMF O'Hare (Chicago), IL 60666-0507 USA

0586-5581/85$1.00+.05

ION DISCRIMINATION EFFECTS IN THE LASER MICROPROBE MASS ANALYZER

Eric Michiels, Marc De Wolf and Renaat Gijbels*

Department of Chemistry, University of Antwerp (U.I.A.)
Universiteitsplein 1, B-2610 Antwerp-Wilrijk, Belgium

(Paper received February 07, 1985: manuscript received June 26, 1985)

Abstract

Different discrimination effects have been observed for atomic and polyatomic cluster ions when varying the ion lens potential of the laser microprobe mass analyzer. This is attributed to the chromatic aberration of the einzel lens, leading to different effects on ions with different energy distributions. Ion kinetic energy distributions were measured using the cut-off property of an ion reflector. The energies of elemental ions are higher and the energy distributions broader than those of polyatomic ions. Chemically different ion species have different energy distributions. An attempt is made to correlate the instrumental effects with results from ray tracing computer programs.

KEY WORDS: Laser Microprobe, Mass Spectrometry, Ion Discriminations, Polyatomic Ions, Kinetic Energy Distributions, Ray Tracing Computer Programs, Ion Transmission.

*Address for correspondence:
R. Gijbels
Department of Chemistry, University of Antwerp,
Universiteitsplein 1, B-2610 Antwerp-Wilrijk,
Belgium Phone No. (32)3 828 25 28

Introduction

The commercial laser microprobe mass spectrometer LAMMA 500 has been described extensively in a number of papers (e.g. Hillenkamp et al., 1975, Kaufmann et al., 1979, Vogt et al., 1981). The laser-induced ions are accelerated towards a time-of-flight mass spectrometer by an electrostatic field which is formed between the sample (at ground potential) and the entrance electrode of the spectrometer (Fig. 1). The latter is situated at a distance of about 5.75 mm from the sample, and the potential usually employed is-3000 V for positive ions, giving an electrical field strength slightly greater than 0.5 V/μm. This configuration can be considered as an ion objective lens which gathers the ions formed from the object into the ion optical system, similar to an optical microscope objective lens. Not all ions are collected and guided through the spectrometer, but the accepted fraction depends on the geometry of the system and the angular ion distribution.

After the acceleration electrode, an "einzel" lens (i.e. a configuration of three electrodes with equal diameter and with the outer electrodes having the same potential, see also Fig. 1) collimates the ion beam in order to improve the transmittance of the mass spectrometer by focussing ions onto the detector that would otherwise be lost to collision with the walls. Specific ion optical characteristics of this lens in the LAMMA 500 have not been published, but ion lenses of this type have been widely employed, and the general design is discussed in many texts on electron optics (e.g. Paszkowski, 1968a, Pierce, 1959, Harting and Read, 1976). Eloy and Dumas (1966) and Eloy (1968) were the first to use an einzel lens in a laser ion source and pointed out that the voltage parameters should be carefully adjusted. These lenses are known to be subject to spherical and chromatic aberrations. Therefore (Mauney, 1984): (a) chemical species of ions will differ in the fraction extracted if they have different distributions in space, (b) if they differ in their distribution of velocity vectors, and (c) sequential measurements will have different fractions of extracted ions, if there is a difference in the spatial distribution of ions formed or in their distribution of velocity vectors.

Two chemical ion species have different

space distributions if, for instance, one is formed primarily in the center of the laser beam, and the other primarily in the lower intensity fringe of the beam. At the same time, since they are formed in regions of different laser intensity, they achieve different initial kinetic energies and thus have different distributions for their velocity vectors. Sequential measurements will differ in both the spatial distribution and velocity distribution of the ions formed if either the specimen geometry or the laser beam profile varies.

It has been stated that atomic ions are principally formed in the intense central region of the laser beam, and that simultaneously molecular ions can be formed by "laser desorption" in the fringe of the beam (Hercules et al., 1982). It was also reported that initial kinetic energy distributions of ions differ from species to species (Hillenkamp et al., 1975, Mauney and Adams, 1984a, Michiels et al., 1984). In each case, the extraction of different classes of ions does not need to be the same and consequently these variations in transmittance interfere with quantitation. In the case of secondary ion mass spectrometry (SIMS), it was found that considerable relative intensity errors could result from the neglect of the relative transmittance of the instrument for the element-specific kinetic energy distribution (Rudat and Morrison, 1979a).

In a previous paper (Michiels and Gijbels, 1983), we reported significantly different intensity dependence of atomic and polyatomic ions from a TiO_2 film on einzel lens voltage (i.e. voltage on the central cylinder of the einzel lens, see also Fig. 1).

The features of these preliminary measurements were attributed to the chromatic aberration of the einzel lens, leading to different transmittance of ions having different energy distributions. In this paper, we discuss the discriminations of the einzel lens for different types of ion species when different laser energies are used. The results are correlated with measurements of ion kinetic energy distributions by using the ion reflector of the laser mass spectrometer (which normally compensates for the spread in ion kinetic energy) as an energy cut-off filter (Michiels et al., 1984). An attempt is made to correlate the results by using ray tracing computer programs.

Materials and Methods

As mentioned above, a detailed description of the laser microprobe mass analyzer LAMMA 500 manufactured by Leybold-Heraeus GmbH (Köln, FR Germany), can be found elsewhere (Hillenkamp et al., 1975, Kaufmann et al., 1979, Vogt et al., 1981). A high-power Q-switched Neodymium-Yttrium Aluminium Garnet (Nd-YAG) laser with frequency quadrupling (λ=265 nm ; τ=15 ns) is focussed onto the sample using an optical microscope, which also serves for visualizing the particle or sample spot to be analysed. The 32 x microscope objective lens was used throughout. The laser-induced ions are accelerated to 3000 V and then collected through an ion optical einzel lens in the drift tube of a time-of-flight (T.O.F.) mass spectrometer, including a "time focussing" ion reflector (U_{refl} = 125 V) for compensating the spread of initial ion energies. In this way, a complete mass spectrum of positively or negatively charged ions is available with every laser shot. The laser pulse energy on the sample can be varied with a set of optical attenuation filters. The ion detection system consists of an open secondary electron multiplier with 17 Cu-Be dinodes (U_{cath}= 6000 V, U_{mult} = 3150 V). The mass spectra were stored without preamplification in a fast transient recorder (Biomation 8100, 20 ns sampling interval, input voltage range between 0.05 and 0.1 V) and fed into a Digital LSI 11/02 microcomputer for mass calibration and peak area calculations using the LAM program package developed in-house (Mauney, 1983). The spectra can be transferred off-line to a Digital VAX 11/780 minicomputer for further data processing.

The specimens consisted of a vacuum-deposited film of TiO_2 (Pulker et al., 1976) on a formvar coated TEM grid obtained by evaporation of Ti_2O_3 tablets during 45 s using a Balzers BA-500 vacuum evaporator.

The ion lens voltage was varied between -850 V (measurements at "low" laser energy) or -800 V (measurements at "high" laser energy) and -1250 V with intervals of 25 V, while the accelerating voltage and the voltage on the T.O.F. electrode were kept constant at -3000 V (Fig. 1). The intensity at a particular lens voltage was obtained as the averaged integrated peak intensities from ten spectra, taken one each from ten preselected grid squares. At least 15 lens voltage settings over the experimental range were selected in random order and the sampled spots were all selected near the center of the grid in order to minimize contributions from instrumental drift or other systematic errors. The first series of measurements was obtained at a "low" laser energy (ca. 0.004 μJ) which yielded similar perforation diameters of about 2 μm in the TiO_2 film. In the second series of measurements at "high" laser energy (ca. 0.01 μJ) the perforation holes were about 4 μm in diameter. Both series were obtained one after the other in less than 150 minutes and a total of 309 mass spectra were recorded for further data processing.

Results and Discussion

The characteristic positive ion mass spectrum obtained by laser irradiation of TiO_2 consists of major peaks from Ti^+ and TiO^+ and a series of less intense polyatomic cluster ions of the type $Ti_mO_n^+$. These features were described extensively by Michiels and Gijbels (1983). In the present context, we are interested in the relative isotope peaks of Ti^+ (m/z = 46,47,48,49,50) and TiO^+ (m/z = 62,63,64,65,66) and in the polyatomic ion peaks at m/z = 81 (TiO_2H^+), 128($Ti_2O_2^+$) and 144 ($Ti_2O_3^+$). Hydrogen adducts, TiH^+ and $TiOH^+$, may contribute to the intensities of all but the lowest isotope peaks of each Ti^+ and TiO^+, the hydrogen probably being derived from adsorbed water and from the formvar support film. Since the low abundant isotope peaks of Ti^+ and TiO^+ on the one hand and the signals of the polyatomic cluster ions on the other hand, have similar in-

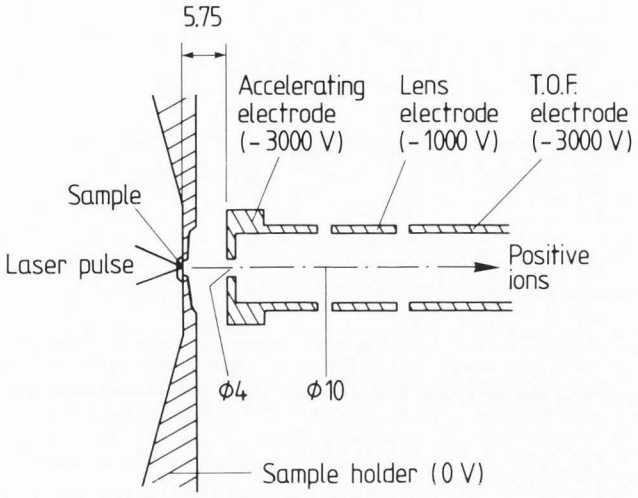

Fig. 1: Scheme of ion source and "einzel" lens in the LAMMA 500. The voltage on the lens electrode ("lens potential") was varied to obtain experimental transmission curves. Distances are given in mm.

tensities, the sensitivity of the transient recorder was adjusted in order to register these intensity signals properly. However, within the selected dynamic range, the intensities of the highly abundant m/z=48 (Ti^+) and m/z = 64 (TiO^+) ion peaks were not measurable. Besides titanium oxide ions a number of element ion peaks at m/z = 23(Na^+), 27(Al^+), 39(K^+) and 40(Ca^+), were present in the mass spectra, probably from contamination during the sample preparation.

In previous measurements (Michiels and Gijbels, 1983) on the same type of sample, the ion lens potential(of the central cylinder of the einzel lens) was varied between -50 and -1850 V (for positive mode mass spectra), while the acceleration potential was kept constant at -3000 V. Over this wide range, the ion intensities of Ti^+ and TiO^+ were both found to vary smoothly, in a similar way; the highest intensities occurred between - 950 and -1350 V, with a maximum at -1050 V (see also Fig. 2). The intensities of the polyatomic cluster ions in the mass range between 40 and 260 amu (e.g. TiO_2H^+, $Ti_2O_2^+$, $Ti_2O_3^+$,$Ti_3O_4^+$) also vary in a similar way but reach a maximum at -1125 V. Consequently, the relative intensities of these complex clusters (relative to Ti^+) differ by more than one order of magnitude at ion lens potentials of -1050 and -1150 V. From -1150 to -1850 V the intensities of the complex cluster ions decrease steadily, in a similar fashion as those of TiO^+ and Ti^+. The decrease in intensity of complex clusters from -1050 to -1000 V is conspicuous (1.5 orders of magnitude): below -950 V the mass lines of $Ti_3O_n^+$, $Ti_2O_n^+$ and TiO_2H^+ can even hardly be observed. The intensities of TiO^+ and Ti^+ also decrease considerably below about -1000 V, but only by one order of magnitude. The decrease is much more slower in the range from -850 to -50 V.

Therefore, in the present experiments we studied the range of ion lens voltages where the variations in spectral intensity are the most pronounced, i.e. between -800 and -1250 V. A shift of 50 to 75 V of the potential axis in comparison

Fig. 2: Mean intensity of various cluster ions from a TiO_2 film as a function of the ion lens potential. The vacuum deposited film was irradiated through the 100x microscope objective and similar perforations in the film of approximately 1.5 µm were obtained.

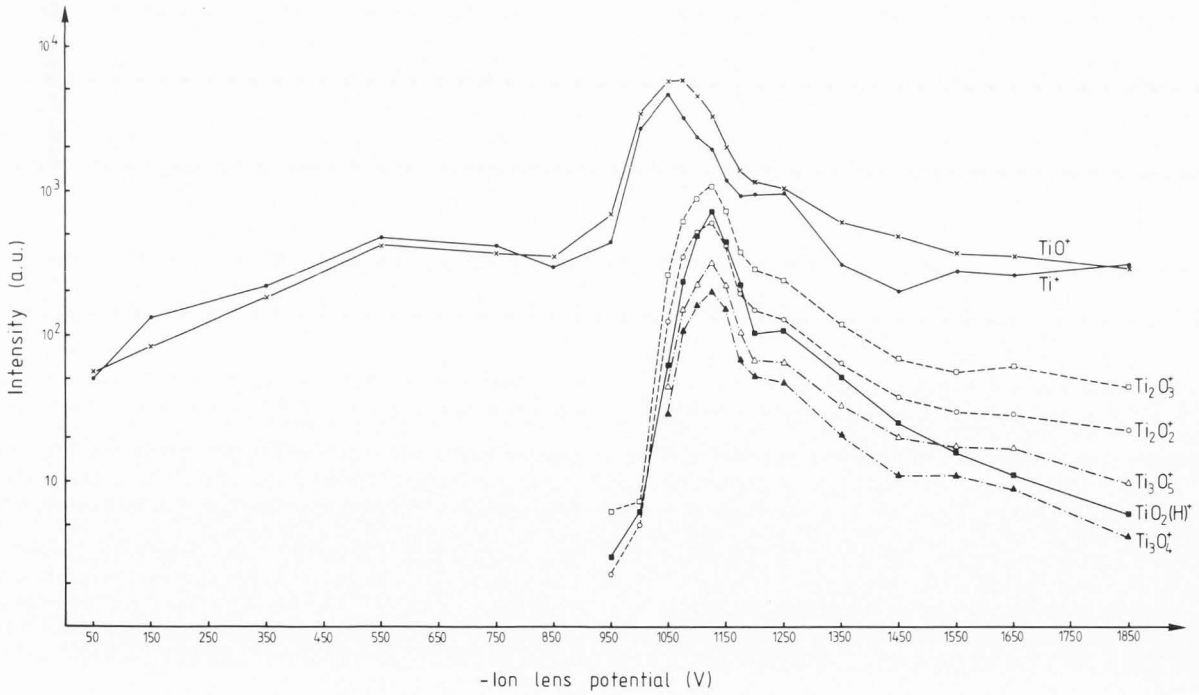

with the previously reported measurements (Michiels and Gijbels, 1983 and Fig. 2) will be noted which is attributed to readings of a non-calibrated high-voltage meter in the earlier experiments. The results obtained at "low" laser energy (ca. 0.004 μJ) are presented in Fig. 3, those at higher laser energy (almost a factor of 3 higher) are given in Fig. 4. Note that in these semi-log plots the intensity of the polyatomic ions at m/z=81, 128 and 144 are drawn relatively to the intensity axis at the right hand side.

For the measurements at "low" as well as at "high" laser energy, the polyatomic cluster ions reach their maximum intensity in the range between -1050 and -1075 V. On the other hand, the maximum intensity of the atomic ions (isotopes of Ti^+) and simple oxide ions (isotopes of TiO^+) is situated at about -1012.5 V in the first series (Fig. 3) and in the range between -925 and -1000 V in the second series (Fig. 4). This means that in each case the intensity maxima between atomic and simple oxide ions on the one hand, and complex polyatomic cluster ions on the other hand, are occurring at different ion lens voltages, with a difference of at least 50 V to more than 100 V depending on the laser energy used. This is in accordance with previous experiments (Michiels and Gijbels, 1983).

The intensity variations in the considered range of lens potentials are similar for both series of measurements. It is striking that at "low" laser energy as well as at "high" laser energy the intensities of all ions vary parallel to each other in the range between -1250 V and about -1075 V. At smaller absolute values of the lens potential (i.e. at larger potential differences between the acceleration voltage and the lens voltage), the polyatomic cluster ions (TiO_2H^+, $Ti_2O_2^+$, $Ti_2O_3^+$) are the first to decrease sharply in intensity, followed by TiO^+ and the atomic ions (Ti^+, Na^+, Al^+, K^+, Ca^+).

If one compares the intensity distributions at the two different laser energies, it is clear that the largest intensity variations appear in the range between -800 V and -1050 V. At higher laser energies, all intensity distributions become broader. This is explicitly shown in Fig. 5 where the intensity variations of some typical ions at "low" and "high" laser energy are superimposed, together with their standard deviations of the mean. This broadening of the intensity distributions is more dominant in the range with small absolute values of the lens potential. The atomic ions appear to be much more subject to these intensity variations as a result of different laser energies, than the polyatomic cluster ions.

When comparing the different intensity variations associated with different types of ions (atomic or cluster ions) it is obvious that the relative intensities of the polyatomic ions (relative to Ti^+) vary considerably depending on the selected ion lens potential. The difference in relative intensity can be two orders of magnitude. This means that by carefully selecting an optimal ion lens potential, it is possible to discriminate against a number of mass spectral interferences which is of importance in view of the limited mass resolution of the time-of-flight mass spectrometer.

The ion discrimination effects of the einzel lens observed above can be attributed mainly to the chromatic aberration of the einzel lens if the different types of ions have different ion kinetic energy distributions. Energy spectra of M^{n+} ions produced by laser pulses have been described for reflection geometry type instruments (Kovalev et al., 1978) but, to our knowledge, the information available for cluster ions, especially for the transmission geometry of the LAMMA 500 instrument, is rather limited. Energy spectra of sputtered ions, including cluster ions, have been studied more extensively, and data for Ti^+, TiO^+, TiO_2^+, Ti_2O^+, $Ti_2O_2^+$, and $Ti_2O_3^+$ were described by Rudat and Morrison (1979b). The energy spectra of polyatomic ions are narrower and peaked at lower energies than the atomic energy spectra, and they decrease in width and average energy with greater ion complexity. The same tendencies can be seen in Fig. 2 to Fig. 5 if the ion energy is assumed to increase from the right to the left. Thus, low-energy ions are predominantly transmitted in the range between -1250 V and about -1075 V, while high-energy ions are still accepted between -1075 to -800 V. The kinetic energy distributions of the elemental ions are expected to be broader and more susceptible to variation in laser energy in comparison with those of the polyatomic ions.

In order to obtain more information, a method for measuring kinetic energy distributions of laser-induced ions was developed in our laboratory, which makes use of the energy cut-off property of the ion reflector (Mauney and Adams, 1984a, Michiels et al., 1984). The ion reflector has an energy filtering effect in addition to its primary function of drift time compensation : ions having a kinetic energy greater than the total potential of the repelling electrostatic field pass through or collide with the reflector grid and are lost. If the reflector is operated as a cut-off filter, the ion energy range of interest can be selected by adjusting the reflector potential. When repetitive spectra are acquired under uniform ionization conditions, stepping of the cut-off level across the energy range provides a measure of the cumulative energy distributions of the ions extracted from the source. Mauney and Adams (1984a, 1984b) reported cumulative kinetic energy distributions of carbon C_n^- cluster ions obtained at different laser energies. The median kinetic energies of these distributions ranged from ca. -5 to -ca. -17 eV. The distributions become broader and more negative with increasing ionic mass. At higher laser energies the median kinetic energies of all the polyatomic ions shift towards more negative values (up to -60 eV).

Cumulative ion kinetic energy distributions for some specific titanium oxide ions (at m/z = 46, 49 (Ti^+); 62, 65 (TiO^+); 40 (Ca^+); 81 (TiO_2H^+); 128 ($Ti_2O_2^+$); 144 ($Ti_2O_3^+$)) are shown in Fig. 6. These distributions were obtained from the same TiO_2 film which was also used during the ion lens experiments and at a comparable "low" laser energy (perforation holes of 2 μm diameter) by varying the ion reflector voltage between -112.5 to +300 V, with intervals of 12.5 V over the negative part of the voltage range. An ion lens potential of ca. -1100 V was selected to maximize the sig-

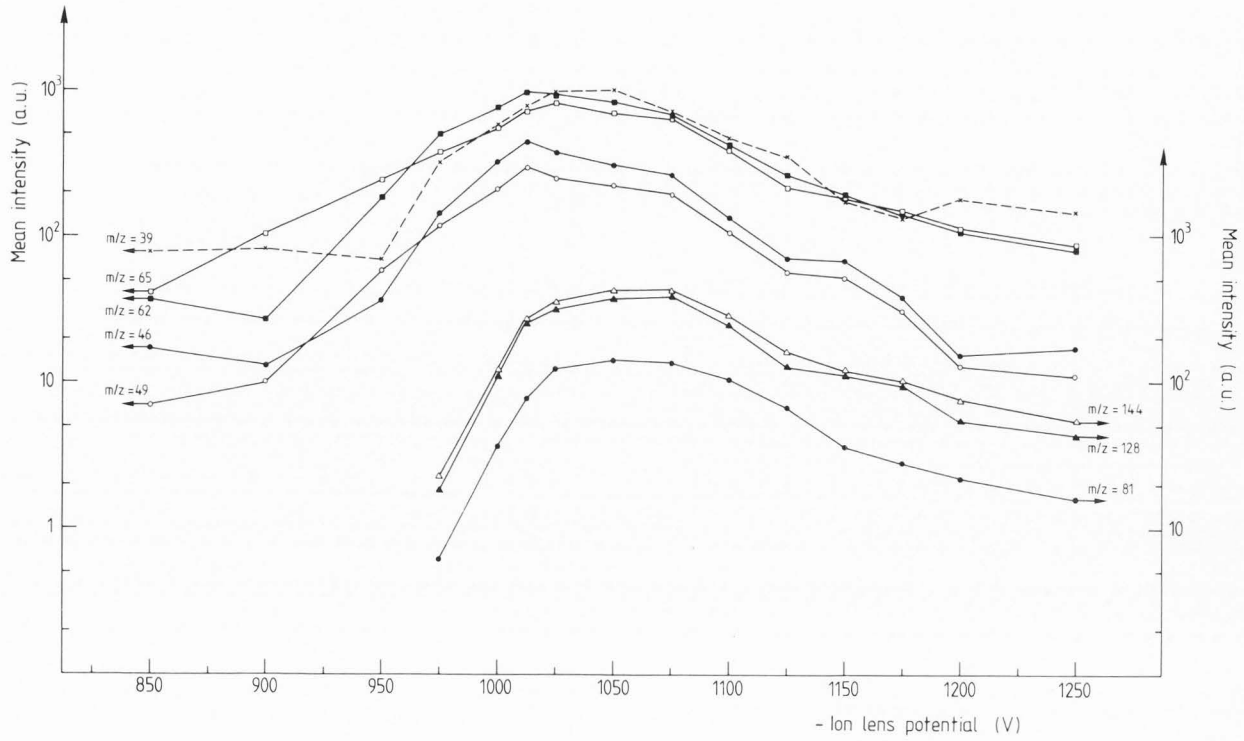

Fig. 3:Mean intensity of some typical atomic and cluster ions from a TiO_2 film as a function of the ion lens potential (m/z = 39 (K^+); m/z = 46, 49 (Ti^+); m/z = 62, 65 (TiO^+); m/z = 81 (TiO_2H^+); m/z = 128 ($Ti_2O_2^+$); m/z = 144 ($Ti_2O_3^+$)). The mass spectra were obtained at a "low" laser energy (ca. 0.004 μJ).

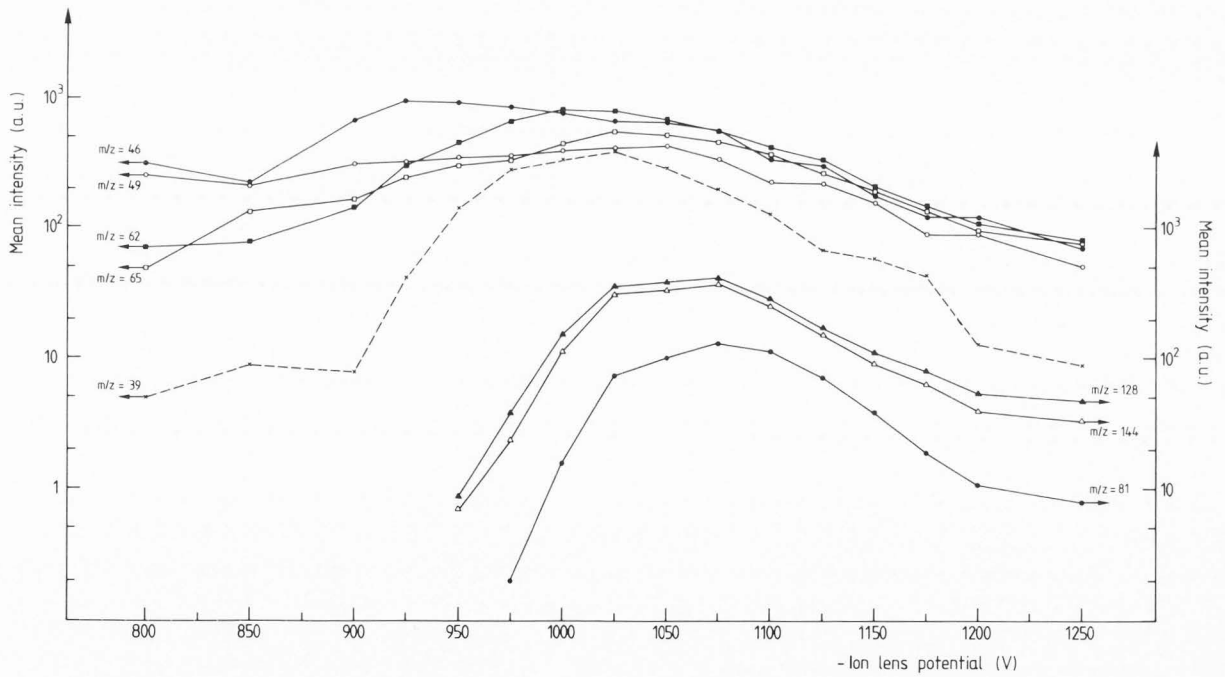

Fig. 4:Mean intensity of some typical atomic and cluster ions from a TiO_2 film as a function of the ion lens potential (m/z = 39 (K^+); m/z = 46, 49 (Ti^+); m/z = 62, 65 (TiO^+); m/z = 81 (TiO_2H^+); m/z = 128 ($Ti_2O_2^+$); m/z = 144 ($Ti_2O_3^+$)). The mass spectra were obtained at a "high" laser energy (ca. 0.01 μJ).

nals for the polyatomic cluster ions. At a sufficiently high voltage setting of the ion reflector (e.g. + 200 V), all singly charged ions of the same mass but with different kinetic energies are reflected and a maximum intensity is observed (plateau-values in Fig. 5). As the reflecting potential is decreased, ions with a high kinetic energy strike the grid or wall so that smaller and smaller fractions of the ions are reflected and the signal decreases. Eventually a potential is reached at which essentially no ions are reflected and no signal is obtained. As can be seen from Fig. 6, ions of a different composition have different intensity variations across the range of reflector potentials, resulting in different positions of the median kinetic energies. Table 1 lists the medians of the distributions obtained by graphical estimates from the 50 % level of hand-drawn smooth curves through the data. In a study with a thermal ion source (Na^+ ions from a heated filament), Mauney and Adams (1985) established that an instrument-dependent correction of the reflector potential by +8 V is required to obtain the actual cut-off ion kinetic energy. This correction has been applied to the tabulated estimates of the distribution medians. The medians shift towards more negative values for more complex (polyatomic) cluster ions, i.e. from Ti^+ (m/z = 46) over TiO^+ (m/z = 62) to $Ti_2O_n^+$ (m/z = 128, 144). Clusters having a hydrogen atom incorporated (e.g. TiO_2H^+ at m/z = 81) yield the most negative value for their median (-25 eV).

The observation that the distributions include negative energy tails and even have negative values for their medians (this means that they have a kinetic energy less than the accelerating potential), is in conflict with the concept that ions are formed from the sample surface having substantial velocities, which are simply added to the electrostatic acceleration into the mass spectrometer. Incomplete acceleration due to the locus of ion formation (i.e. when ions are formed after some expansion of the vapour) or energy-reducing collisions of ions traversing the vapour cloud are considered to be the most probable explanations for the observation of negative distribution medians. If the observed deficiency of kinetic energy is principally related to the fraction of the accelerating potential experienced by an ion after its formation, then the median kinetic energies can be related to chemical effects, interpreting the order of increasing deficiency as indicative of delay in ion formation in an expanding plasma.

Since $^{46}Ti^+$ has the most positive distribution, which is at the same time the least sharply inflected of those observed (Table 1 and Fig. 6), this is an indication that $^{46}Ti^+$ was the earliest formed with a wide spread of kinetic energies. A large spread would be consistent with formation at high thermal energies followed by transfer of energy to other species in the plasma cloud. The oxide ions m/z = 62 (TiO^+), 128 ($Ti_2O_2^+$) and 144($Ti_2O_3^+$) have medians which are 25 to 30 eV more negative than for ions at m/z = 46 (Ti^+). This would imply formation after plasma expansion by about 50 to 60 μm, occurring by vapour-phase ion formation processes rather than direct formation from the solid (the field strength in the ion source is ca. 0.5 V/μm).

Table 1: Median values of kinetic energy distributions for atomic and cluster ions from a TiO_2 film.

m/z	median (eV)	m/z	median (eV)
46	10	40	0
49	-15		
		81	-25
62	-15	128	-20
65	-25	144	-20

The distributions of the heavier isotopes of Ti^+ and TiO^+ are different from those of the lightest isotope and their median kinetic energy appears to be shifted towards more negative values (Fig. 6 and Table 1). The magnitude of this discrimination is illustrated more clearly in plots of kinetic energy probability distributions (Fig. 7). These are obtained by differentiating hand-drawn cumulative ion kinetic energy distributions through the experimental data. The kinetic energy distributions of the m/z = 65 ion species appear clearly as a composite of two components, which are most probably titanium oxide and hydroxide. Also the m/z = 49 kinetic energy distribution is shifted towards more negative energy values : this can be attributed to the presence of titanium hydride (TiH^+).

The m/z = 81(TiO_2H^+), 128($Ti_2O_2^+$) and 144 ($Ti_2O_3^+$) energy distributions are much narrower and have practically no higher-energy tails. In this interpretation of ion kinetic energy distributions, the width of the distribution is indicative of the depth of the formation region in the plasma as well as the velocities of the particles involved in the formation reaction. The kinetic energy distribution of the atomic ions may include contributions from both the formation locus and from ejection of ions formed initially in the laser impact region. The larger cluster ions of titanium dioxide progress to narrower distributions, suggesting that the range of conditions favourable for their formation is narrower than for the small ions. According to the most probable kinetic energies displayed in Fig. 7, the order of ion formation in the expanding plasma would be roughly: Ti^+, $TiO^+ \approx TiH^+$, $Ti_2O_2^+ \approx Ti_2O_3^+$, TiO_2H^+, $TiOH^+$.

These measurements of kinetic energy distributions of different types of ions (atomic or cluster ions) confirm the features observed in the experiments in which the ion lens potential was varied. The energy distributions of the elemental ions appear to be much broader and have a high-energy tail in comparison with those of the polyatomic cluster ions. At higher laser energies, the kinetic energy distributions of all ions become broader, but to a greater extent for those of the atomic ions (Michiels et al., 1984).

Recently, a study was started to calculate the ion transmission of the LAMMA 500 using ray tracing computer programs, in order to verify the experimental results obtained by varying the ion lens voltage and in particular the different

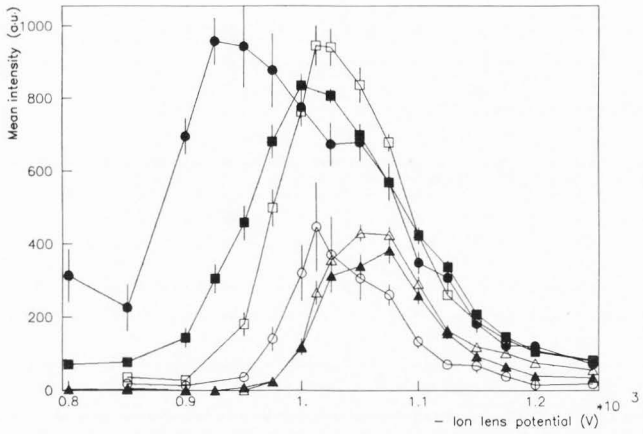

Fig. 5:Intensity variations as a function of the ion lens potential, with standard deviations of the mean, at "low" (O: m/z = 46 (Ti^+); □: m/z = 62 (TiO^+); △: m/z = 144 ($Ti_2O_3^+$)) and at high (●: m/z = 46 (Ti^+); ■ m/z = 62 (TiO^+); ▲m/z = 144 ($Ti_2O_3^+$)) laser energy.

variations observed between atomic and polyatomic ions (see also above). To describe ion optical systems adequately a number of partial differential equations have to be solved in order to obtain the electric field distribution, which allows one to describe the behaviour of charged particles. However, the equations being of the elliptic type, they cannot be solved under all circumstances. Instead of trying to look for an analytical solution, the problem can also be approximated by using finite-difference methods. This led to the well-known Liebmann relaxation technique (e.g. Paszkowski, 1968b) which is very handy if a computer is available. The method is based on the superposition of a net upon the region of interest. It can be shown that the potential of a mesh point is a function of the potential of its neighbours. The obtained set of equations is solved iteratively starting from a trial solution. Each successive approximation will decrease the error of the calculated values until some accuracy requirement is met.

The above outlined procedure was actually used to make a simulation of the electric field in the ion lens of the LAMMA 500. A program (W126) of the European Organization for Nuclear Research (CERN) Computer Center tackled Laplace's equation by making use of a two-dimensional approach. Afterwards the same program could be used to calculate the ion trajectories. Starting from some specified location with a definite slope and initial kinetic energy, the particles trajectory is again iteratively calculated with a numerical method of integration. No space charge effects were taken into account, so the motion obeys the equation:

$$\frac{d^2r}{dz^2} = \frac{1 + \left(\frac{dr}{dz}\right)^2}{2\,\emptyset\,(z,r)} \left\{ \frac{\delta\emptyset(z,r)}{\delta r} - \frac{dr}{dz}\,\frac{\delta\emptyset(z,r)}{\delta z} \right\} \quad (1)$$

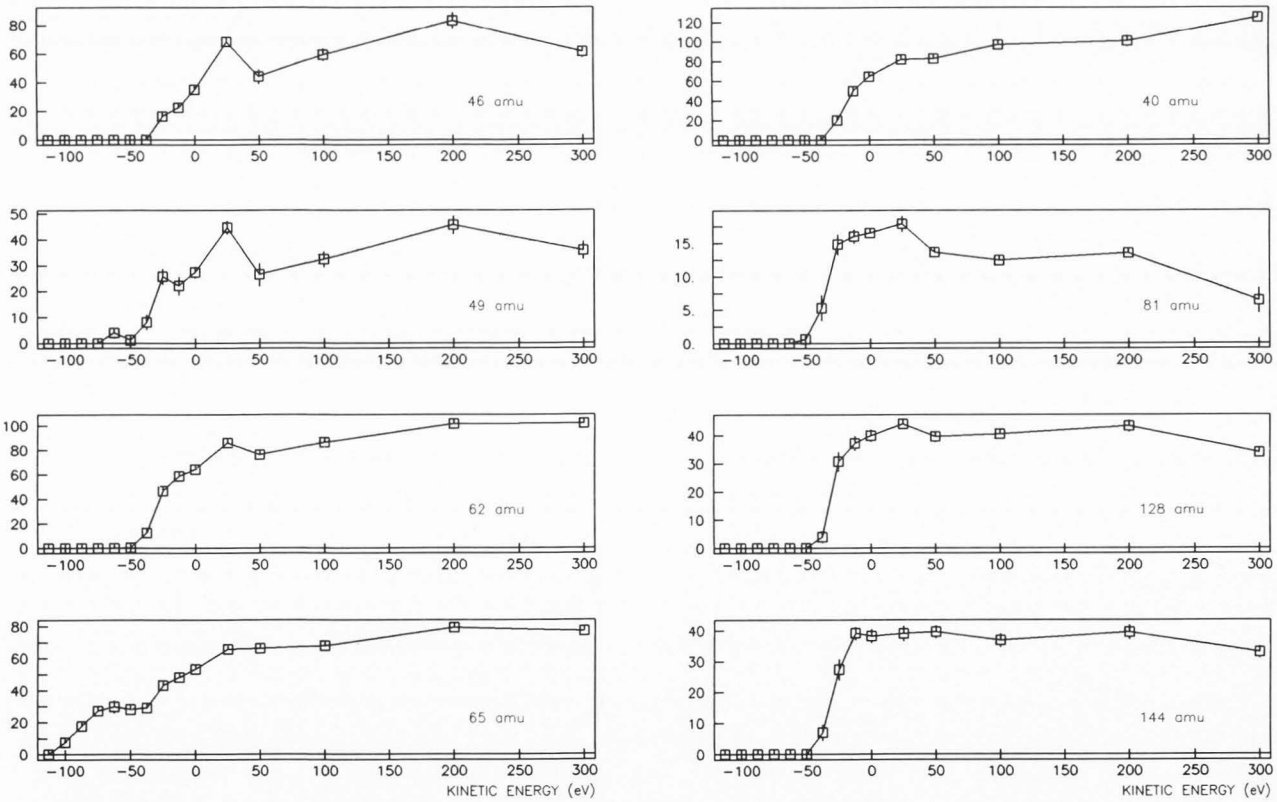

Fig. 6:Cumulative ion kinetic energy distributions of singly charged atomic and cluster ions from a TiO_2 film (46, 49 amu: Ti^+; 62, 65 amu: TiO^+; 40 amu: Ca^+; 81 amu: TiO_2H^+; 128 amu:$Ti_2O_2^+$;144 amu: $Ti_2O_3^+$).

with ϕ (z,r) being the potential at the position with cylindrical coordinates (z,r).

After obtaining the ion paths through the einzel lens, the motion in the remaining part of the instrument could be easily determined. Apart from two drift spaces characterised by a definite rectilinear motion, a reflector area is situated between them. For this electrostatic mirror the following equations are valid :

$$r_{out} = r_{in} - \frac{4k\ E_{in}}{\Delta V} \sin \phi_{in} \cos \phi_{in} \qquad (2)$$

$$\phi_{out} = - \phi_{in} \qquad (3)$$

$$E_{out} = E_{in} \qquad (4)$$

where the optical axis is chosen to coincide with the z-axis and the starting coordinates are (o,r_{in}) at t=o. The particle enters under a direction ϕ_{in} with a kinetic energy E_{in}. $\Delta V/k$ is the electric field strength in the reflector with length k.

To summarize : with the above routines it can be decided whether an ion created at or nearby the specimen's surface will or will not be detected by the electron multiplier located at the end of the second drift tube. In other words, it is possible to calculate the transmission for an ion of interest as a function of adjustable electrode voltages and assuming acceptable angular and energy distributions.

Using these computer programs, radii (with respect to the optical axis) were calculated at 100 mm from the detector at the end of the second drift tube. At this position, all rays which have an r-value less than 18.75 mm from the optical axis will be post-accelerated towards the cathode of the electron multiplier and are detected. This was checked with the computer program W126. The programs allow changes in initial kinetic energy, position of departure (i.e. position of ion formation), emittance angle and potential field. Fig. 8 shows the radii (100 mm in front of the detector) for ions having an initial kinetic energy of 5 eV and which are emitted at the position of the sample surface, on the optical axis, and with different emittance angles. The radii are calculated for different ion lens voltages. Thus, ions emitted at an angle of e.g. 22.5° will be detected in the range of lens voltages between ca. -650 and -1040 V since the rays are situated within an area with a diameter of 37.5 mm. If an integration is made of all possible emittance angles, initial kinetic energies and positions of departure and if a suitable distribution for each of these parameters is taken into account, the resulting ion transmission can be calculated as a function of the ion lens voltage.

However, information about angular and kinetic energy distributions is rather scarce, while data on positions of ion formation and corresponding space distributions are practically non-existent. Therefore, a number of suppositions are required. For the angular dependence, we used isotropic, $\cos \theta$ and $\cos^2 \theta$ distributions. According to the literature, $\cos \theta$ and $\cos^2 \theta$ distributions are frequently measured for atomic ions when using a reflection geometry for laser excitation and ion extraction (e.g. Ready, 1971, Dinger et al., 1980). However, there is no physical reason for an equivalent angular dependence between the laser reflection absorption mode and transmission absorption mode : the expansion of plasma is monodirectional in the first configuration and bidirectional (?) in the second one. For polyatomic ions no information at all could be found for either geometry. We also assume that for instance all atomic Ti^+ ions formed with different kinetic energies, have the same angular distributions. Ray trajectories are calculated for emittance angles between 0° and 85° (i.e. at 2.5°; 7.5°; 12.5°;...; 82.5°) assuming a perfect cylindrical geometry.

Since there does not exist any information on kinetic energy distributions which are corrected for transmission in the LAMMA 500, we used the distributions as measured with the ion reflector (see also above and Fig. 7). Furthermore, we assumed that the distributions start at 0 eV instead of a "negative" energy value. Ray trajectories are calculated for ions having an initial kinetic energy between 0 and 50 eV, with intervals of 10 eV (i.e. at 5 eV, 15 eV, 25 eV, 35 eV and 45 eV).

The calculations were carried out for rays starting at the sample surface and on the optical axis. In a further study ray trajectories will be calculated for rays on the optical axis but starting at some distance from the sample surface. The latter situation would reflect ion formation (mostly polyatomic) after plasma expansion (see also above). Radii were calculated as a function of the ion lens voltage between -500 and -1400 V, while the accelerating voltage was kept constant at -3000 V. In these theoretical calculations, it is also assumed that the field lines are not disturbed by a shielding effect of the plasma.

Fig. 9 shows the calculated transmission (on a logarithmic scale) as a function of the ion lens voltage for $^{46}Ti^+$. The kinetic energy distribution of Fig. 7 was used, an angular $\cos^2 \theta$ distribution was assumed and all rays started at the sample on the optical axis. This transmission curve should be compared with the experimentally obtained transmission of $^{46}Ti^+$ ions as a function of the ion lens voltage (Fig. 3). The calculated transmission appears to be broader and its maximum is situated at a lower lens potential (ca. -950 V). On the other hand, if we use and isotropic angular distribution instead of the $\cos^2 \theta$ distribution, the position of maximum calculated transmission shifts slightly towards higher lens voltages while the right hand side of the curve becomes more enhanced and less steep than the left hand side. This is in better agreement with the experimentally obtained transmission curve.

The influence of the ion kinetic energy (we used the kinetic energy distribution of $^{144}Ti_2O_3^+$ (Fig. 7) instead of the distribution of $^{46}Ti^+$) on the transmission curve is also more pronounced at the right hand side of the curve. This is in conflict with the assumption that the substantial intensity differences in the range at low lens voltages are due to the different kinetic energy distributions of e.g. Ti^+ and $Ti_2O_3^+$ (see also Fig. 5). However, up till now the ion trajectories were all calculated for rays starting at the position of the sample. It is not clear what the influence will be if some kind of spatial dis-

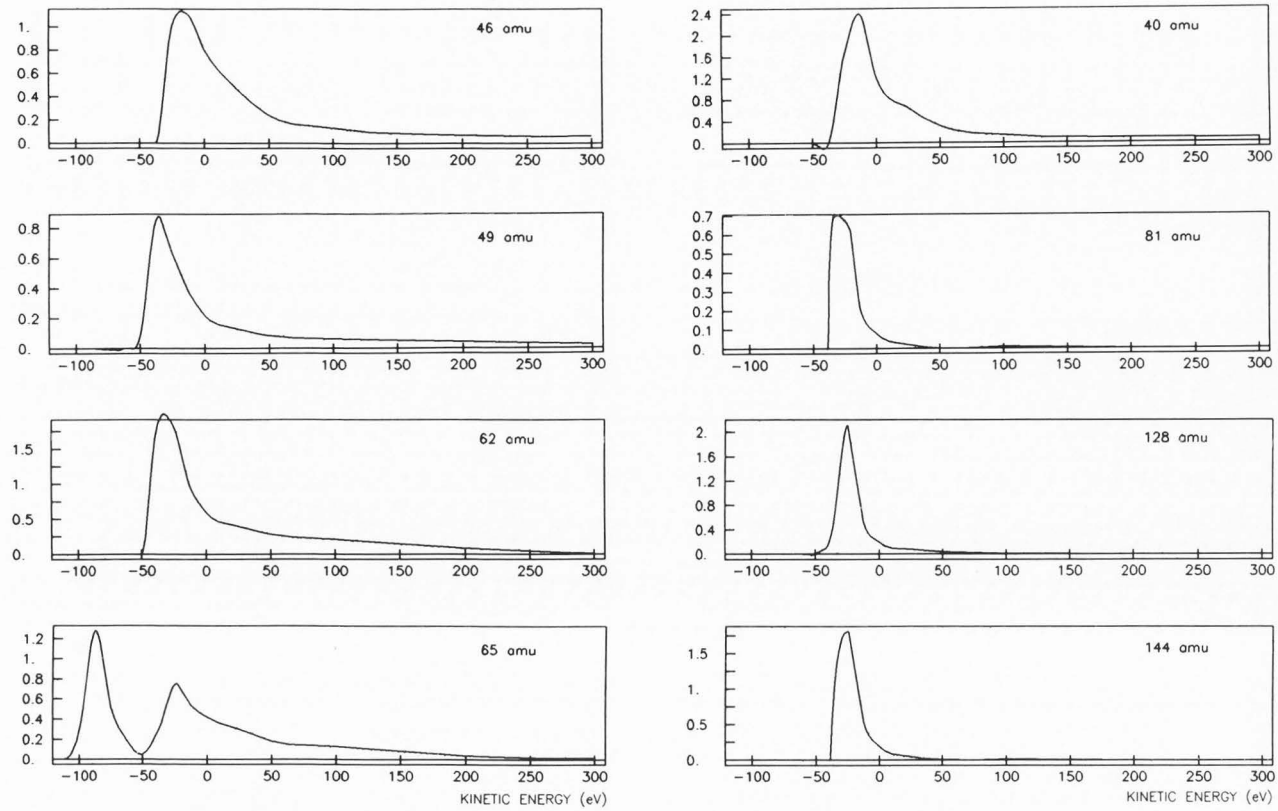

Fig. 7:Ion kinetic energy distributions of singly charged atomic and cluster ions from a TiO_2 film obtained by differentiating cumulative distributions (46, 49 amu: Ti^+; 62, 65 amu: TiO^+; 40 amu: Ca^+; 81 amu: TiO_2H^+; 128 amu: $Ti_2O_2^+$; 144 amu: $Ti_2O_3^+$).

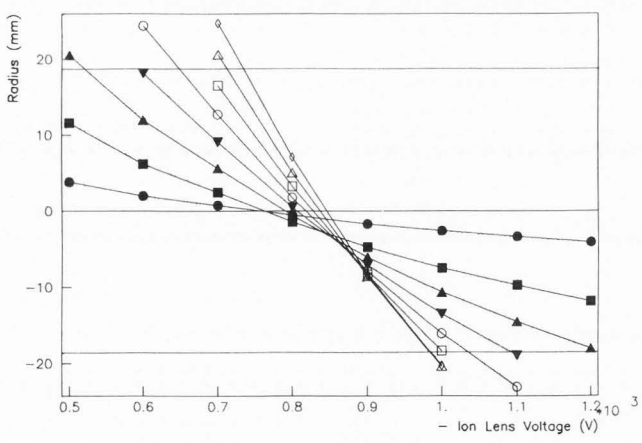

Fig. 8:Calculated radii (with respect to the optical axis in the second drift tube of the LAMMA 500) of ion trajectories as a function of the ion lens voltage, for ions having an initial kinetic energy of 5 eV and which are emitted at the sample surface, on the optical axis, with emittance angles of 2.5° (●), 7.5° (■), 12.5° (▲), 17.5° (▼), 22.5° (○), 27.5° (□), 32.5° (△) and 37.5° (◇). Radii within an area with a diameter of 37.5 mm will be detected by the electron multiplier (see also text).

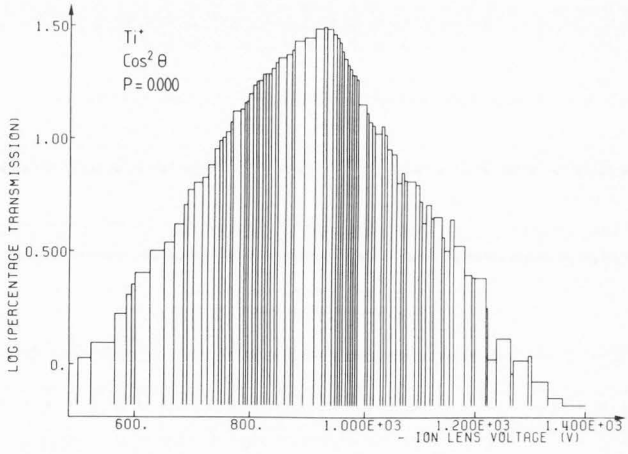

Fig. 9:Calculated percentage transmission (on a logarithmic scale) as a function of the ion lens voltage for $^{46}Ti^+$ ions (see also text).

tribution for ion formation is taken into account, i.e. if the ions are considered as formed at different positions from the sample surface. Further study is also needed to check whether ions with a low kinetic energy should have a different angular distribution than the same type of ions but having a higher kinetic energy (e.g. an isotropic

angular distribution instead of a $\cos^2 \theta$ distribution, respectively). By judiciously adjusting these parameters, it is probably possible to obtain a better accordance between the calculated and experimentally obtained transmission curves.

Conclusions

Using a homogeneous TiO_2 film, it was found that different discrimination effects appear as a function of the ion lens potential of the LAMMA 500. Relative intensities associated with different types of ions (atomic or cluster ions) can differ by two orders of magnitude depending on the selected ion lens potential. This allows discrimination against mass spectral interferences. When different laser energies are used, the largest influence on the intensity distributions is situated in the range of ion lens potentials between -800 and -1050 V. These discrimination effects were attributed mainly to the chromatic aberration of the einzel lens, leading to different effects on ions with different energy distributions.

By using the drift-time correcting ion reflector as an energy cut-off filter, different energy distributions for atomic versus polyatomic ions were indeed obtained. It appeared that the energies of the elemental ions are higher and the energy distributions broader than those of the polyatomic cluster ions. The observation that the kinetic energy distributions include negative energy tails and even have negative values for their medians, can principally be related to the fraction of the accelerating potential experienced by an ion after its formation or to energy-reducing collisions of ions traversing the vapour cloud. This would imply cluster ion formation during plasma expansion, occurring by vapour-phase ion formation processes rather than direct formation from the solid.

In an attempt to explain the experimental results, theoretical ion transmission curves were calculated as a function of the ion lens potential with ray tracing computer programs. Using suitable distributions for all possible emittance angles and initial kinetic energies, the resulting ion transmission could be obtained for ions with a position of departure (i.e. position of ion formation) on the optical axis, at the sample surface. The best similarities between theoretical and experimental transmission curves were found when assuming that elemental Ti^+ ions are formed predominantly at the sample surface with an isotropic angular distribution. Further study is in progress to calculate transmission curves for ions with a departure position at a certain distance from the sample surface; in this way a better agreement with the experimental transmission curves is obtained for the polyatomic ions.

Acknowledgement

The authors thank Dr. T. Mauney for stimulating discussions and initial implementation of the computer programs. This work was supported by the Interministrial Commission for Science Policy, Belgium, through research grant 80-85/10. The secretarial skill of Miss Tania Beyers is gratefully acknowledged.

References

Dinger R, Rohr K, Weber H. (1980). Ion distribution in laser produced plasma on tantalum surfaces at low irradiances. J. Phys. D: Appl. Phys. 13, 2301-2307.

Eloy JF. (1968). Nouvelles expériences au spectromètre de masse à source laser. Méthod. Phys. Anal. 2, 161.

Eloy JF, Dumas JL. (1966). Etudes des ions produits par impact laser dans une source de spectromètre de masse. Méthod. Phys. Anal. 3, 251-256.

Harting E, Read FH. (1976). Electrostatic Lenses, Elsevier, New York, 111-172.

Hercules DM, Day RJ, Balasanmugam K, Dang TA, Li CP. (1982). Laser microprobe mass spectrometry 2. Applications to structural analysis. Anal. Chem. 54, 280A-305A.

Hillenkamp F, Unsold E, Kaufmann R, Nitsche R. (1975). A high-sensitivity laser microprobe mass analyzer. Appl. Phys. 8, 341-348.

Kaufmann R, Hillenkamp F, Wechsung R, Heinen HJ, Schürmann M. (1979). Laser microprobe mass analysis: Achievements and aspects. Scanning Electron Microsc. 1979; II: 279-290.

Kovalev I, Maksimov G, Suchkov A, Larin N. (1978). Analytical capabilities of laser probe mass spectrometry. Int. J. Mass Spectrom. Ion Phys. 27, 101-137.

Mauney T. (1983). LAM, Laser Mass Spectrometry Data System, Program and Users' Guide, University of Antwerp, internal report, 66 pp. (available at UIA).

Mauney T. (1984). Instrumental effects in LAMMA, measurements of kinetic energy distributions and analysis of soot particles. Doctoral Thesis, Colorado State University, Fort Collins, U.S.A.

Mauney T, Adams F. (1984a). Ion kinetic energy measurements on laser induced plasmas in laser microprobe mass analysis (LAMMA). Part 1. Methodology. Int. J. Mass Spectrom. Ion Processes 59, 103-119.

Mauney T, Adams F. (1984b). Interpretation of ion kinetic energy distributions in laser microprobe mass analysis, in: Microbeam Analysis-1984, A.D. Romig Jr. and J.I. Goldstein (eds), San Francisco Press, San Francisco, 19-22.

Mauney T, Adams F. (1985). A simple thermal ion source for examination of a laser ionization mass spectrometer. Int. J. Mass Spectrom. Ion Processes 63, 201-216.

Michiels E, Gijbels R. (1983). Fingerprint spectra in laser microprobe mass analysis of titanium oxides of different stoichiometry. Spectrochim. Acta 38B, 1347-1354.

Michiels E, Mauney T, Adams F, Gijbels R. (1984). Ion kinetic energy measurements on laser induced plasmas in laser microprobe mass analysis (LAMMA). Part 2. Titanium dioxide. Int. J. Mass Spectrom. Ion Processes 61, 231-246.

Paszkowski B. (1968a). Electron Optics, American Elsevier Publishing Co. Inc., New York, 211-218.

Paszkowski B. (1968b). Electron Optics, American Elsevier Publishing Co. Inc., New York, 77-87.

Pierce JR. (1959). Theory and Design of Electron Beams, Van Nostrand, New York, 92-115.

Pulker HK, Paesold G, Ritter E. (1976). Refractive indices of TiO_2 films produced by reactive evaporation of various titanium-oxygen phases. Appl. Opt. 15, 2986-2991.

Ready JF. (1971). Effects of high-power laser radiation, Academic Press, New York, 154-155.

Rudat MA, Morrison GH. (1979a). Discrimination effects in SIMS. Part III. Ion optical and energy discrimination. Int. J. Mass Spectrom. Ion Phys. 32, 53-65.

Rudat MA, Morrison GH. (1979b). Energy spectra of ions sputtered from elements by O_2^+ : A comprehensive study. Surf. Sci. 82, 549-576.

Vogt H, Heinen HJ, Meier S, Wechsung R. (1981). LAMMA 500 principle and technical description of the instrument. Z. Anal. Chem. 308, 195-200.

Discussion with Reviewers

N.S. Mc Intyre : Does the different lens focussing behaviour of TiO^+ compared with oxide clusters of higher molecular weight suggest that these latter may originate at a different time in the ion formation process ?
D.S. Simons : What time difference would be associated with a 50 to 60 μm expansion of the plasma? If two species with the same m/z, e.g. Ti(49)O and Ti(48)OH, were formed at different times, might they be resolvable in the TOF mass spectrum as a result of the time difference in ion formation?
Authors : Since the ion lens is subjected to both spherical and chromatic aberrations, chemical species of ions can be extracted to a different extent if they have different distributions in space. If this is the case, it is reasonable to assume that, indeed, they originate at different times. The observations of negative energy medians for kinetic energy distributions obtained by using the ion reflector as an energy cut-off filter, suggest that polyatomic ions were formed after plasma expansion by about 50 to 60 μm. At an electric field strength of 0.5 V/μm, ions of m/z = 65 would require 10 to 15 ns to cross that distance. This time difference in ion formation will not be resolved in the TOF mass spectrum when using the ion reflector for compensating differences in initial kinetic energy and hence in time of ion formation (ions formed at a later stage originate in a "cooler" environment, and have, on the average, lower kinetic energies, the more so as they experience incomplete acceleration). However, when using a linear time-of-flight mass spectrometer, peak shoulders were observed in the mass spectra at m/z = 65 and 66 which could be interpreted as being due to delayed ion formation (Michiels, 1985).

D.S. Simons : The trend of carbon cluster ion kinetic energy distributions to become broader with increasing ion mass is opposite to what is generally found in SIMS. Any explanation?
Authors : The width of ion kinetic energy distributions as measured with the ion reflector by using its cut-off filter property, can be interpreted as indicative of the depth of the ion formation region as well as of the velocities of the particles involved in the formation reaction. If ions can be formed in a large region (i.e. at certain distances from the sample surface), some of them will be incompletely accelerated resulting in broad kinetic energy distributions. The trend in widths of kinetic energy distributions of carbon cluster ions suggests that in LAMMA the larger ions can be formed under a greater range of conditions than the smaller ones (Mauney and Adams, 1984a).

D.S. Simons : Why should the kinetic energy distribution of elemental ions be more susceptible to variations in laser energy compared with those of polyatomic ions?
J.-F. Eloy : Can you explain why atomic and polyatomic ions reach intensity maxima at different ion lens potentials, depending on the laser energy used?
Authors : If atomic ions are mainly formed in the high energy region of the laser-solid interaction, then the laser energy will directly influence their kinetic energy, e.g. high laser energy will yield high ion kinetic energies and broad energy distributions. If polyatomic ions are formed after cooling of the plasma to sufficiently low temperature, then their kinetic energy will be characteristic for these conditions, i.e. lower kinetic energies and narrower distributions, and hence be less dependent on the initial laser energy. Any difference in energy distributions also has an effect on the experimental transmission curves as a function of the ion lens voltage : the transmission curves of polyatomic ions are therefore less dependent on the laser energy than those of elemental ions (see also Fig. 5).

J.-F. Eloy : The ion reflector compensates the spread of initial ion energies. To what extent will the results of this work be disturbed by the function of electrostatic filter of the ion reflector?
Authors : Since the ion reflector voltage was fixed at 125 V for the measurements of the ion intensities as a function of ion lens voltage, nearly all ions will be reflected. This can also be seen in Fig. 6 : all intensity signals have practically reached a plateau value at reflector voltages between 0 and 100 V.

D.S. Simons : From isotopic measurements can you estimate the relative magnitude of Ti(48)H versus Ti(49) and Ti(48)OH versus Ti(49)O?

Authors : We compared the intensity ratios of m/z = 46 relative to m/z = 49 and of m/z = 62 relative to m/z = 65 with the natural abundance ratio 46/49 which is ca. 1.44. For the measurements at "low" laser energy and ion lens voltages between -850 and -1250 V, the relative magnitude of Ti(48)H versus Ti(49) is ca. 5 % and for Ti(48)OH versus Ti(49)O it is ca. 30 %. For the measurements at "high" laser energy and ion lens voltages between -800 and -1250 V, there is no enhancement of the m/z = 49 signal relative to the m/z = 46 signal while the relative magnitude of Ti(48)OH versus Ti(49)O is only 10 %.

J.-F. Eloy : Which are the considered isotopic masses in Fig. 2 ? What is the number of measurements for each experimental point? What is the error of each measured value ?
Authors : The intensities in Fig. 2 are the sum of all isotopic ion peaks belonging to the same type of ion. Each experimental point represents the average intensity from 5 to 7 mass spectra. The relative standard deviations are typically between 10 and 20 % for the most intense peaks in the mass spectra and rise to more than 50 % for the low intensity signals of polyatomic ions.

D.S. Simons : The range of intensities in Fig. 2 covers about 3 decades. How was this recorded with an 8-bit digitizer ?
Authors : Between ion lens potentials of -1000 and -1125 V for Ti^+ and between -1000 and -1250 V for TiO^+, the highly abundant isotope peaks at m/z = 48 and 64 respectively were too intense to be measured. For these potential regions the two less abundant isotopes of Ti^+ and TiO^+ having the smallest m/z (i.e. at m/z = 46, 47 and 62, 63 respectively) were selected to calculate the ion intensity of the m/z = 48 and 64 ion peaks. This was done on the basis of the averaged contribution of these less abundant ion peaks to the total intensity of the Ti^+ and TiO^+ ion signals in the remaining range of ion lens potentials. This contribution was about 20 %. The deviation from the natural abundance of ^{46}Ti and ^{47}Ti (together ca. 15 %) is also a result of the limited dynamic range of the transient recorder (Simons, 1983).

J.-F. Eloy : What are the accuracy and reproducibility of the "low" and "high" laser energies ? What is the laser energy threshold to obtain perforation of the TiO_2 film ?
Authors : Since the photodiode energy meter was calibrated with a pyro-electric energy meter a few months after the experiments, it is very difficult to state the accuracy of the given laser energy values. Measurements after calibration of the photodiode meter indicated that at least the order of magnitude of the given laser energy values is correct. The reproducibility of the photodiode energy meter readings for a number of sequential laser shots is ca. 10 to 20%. Perforations of about 2 μm in diameter were obtained at 2 to 3 times the threshold laser energy for perforation of the TiO_2 film and detection of ion signals. The measurements at "high" laser energy (diameters of 4 μm) were taken at 5 to 6 times this threshold energy.

J.-F. Eloy : No space charge effects were taken into account when calculating the particles trajectories, why ? Space charge effects appear certainly in the case of the "high" laser energy.
Authors : Without any doubt, space charge effects appear, especially in the case of "high" laser energy. However, for the present preliminary calculations, this effect was disregarded : we have, indeed, already incorporated in our model a number of parameters, for which no experimental data are available (e.g. angular distribution, position of ion formation). To include such parameters as ion/electron current density, beam shape and ion/electron current density distribution (spatial density profile of the plasma as a function of time), which control the space-charge repulsion and electrical field modification, would, at the present time, yield an unwieldy model, with too many unknown quantities.

J.-F. Eloy : From the results of the experimental determination of ion lens voltage threshold for each ion disappearing in the mass spectra, doesn't the computer program allow the determination of each experimental emission angle ?
Authors : The experimental transmission curves are the result of a combination of different parameters each having a different influence. These parameters are the distributions of the initial kinetic energy, the emittance angle and the position of departure. Therefore it is not possible to correlate directly experimental results with just one parameter such as the emission angle (angular distribution).

Additional References

Michiels E. (1985). Instrumentele effecten in laser microprobe massa analyse en clusterionen distributies van oxiden en fluoriden. Doctoral Thesis, University of Antwerp, Antwerp, Belgium.

Simons DS. (1983). Isotopic analysis with the laser microprobe mass analyzer. Int. J. Mass Spectrom. Ion Processes 55, 15-30.